Organic & Biomolecular Chemistry

Accepted Manuscript

ROYAL SOCIETY OF CHEMISTRY

www.rsc.org/obc

Cite this: DOI: 10.1039/c0xx00000x

www.rsc.org/xxxxxx

ARTICLE TYPE

Large dipole moment to promote gelation for 4-nitrophenylacrylonitrile derivatives with gelation-induced emission enhancement property

Pengchong Xue,*[a] Boqi Yao,[a] Yuan Zhang,[b] Peng Chen,[d] Kechang Li,[c] Baijun Liu,[c] Ran Lu,*[a]

Received (in XXX, XXX) Xth XXXXXXXXX 20XX, Accepted Xth XXXXXXXXX 20XX

DOI: 10.1039/b000000x

A series of 4-nitrophenylacrylonitrile and phenylacrylonitrile derivatives consisting of carbazole moiety was synthesized. Some of these derivatives with longer alkyl chains and nitro group could gelatinize some organic solvents, such as ethanol, *n*-butanol, ethyl acetate, and DMSO. By contrast, phenylacrylonitrile derivatives did not form gels in measured solvents. This result proved that the electron-withdrawing nitro moiety was important for gel formation because it conferred the molecules with large dipole moments, which enhanced intermolecular interaction. Analyses by UV–vis absorption, X-ray diffraction, and scanning electron microscopy showed that the gelator molecules could self-assemble into one-dimensional nanofibers with layer packing, which further twisted into thicker fibers and formed three-dimensional networks in gel phase. The single crystal structure of **C4CNPA** implied that the gelators might adopt an anti-parallel molecular stacking because of their larger ground-state dipole moment. Interestingly, the organogels had enhanced fluorescence relative to solutions at the same concentration.

Introduction

Researchers and engineers have significantly focused on stimulus-active functional materials because these materials can change their physical or chemical properties upon exposure to particular stimuli, such as heat, electricity, light, magnetic, solvent, and pH value.[1] These unique characteristics enable stimulus-active materials to be used in many fields, such as smart textiles and apparels, intelligent medical instruments and auxiliaries, artificial muscles, biomimetic devices, heat shrinkable materials, self-deployable sun sails in spacecrafts, miniature manipulators, actuators, and molecular motors and sensors. In particular, smart functional organogels, formed by a large amount of organic solvents and a small amount of low-molecular mass compound with low concentration, have been widely developed in recent years. Their bulk shape and properties can be either switched or tuned by an external chemical or physical stimulus, such as metal ions, anions, small organic compounds, protons, light irradiation, oxidation or reduction reaction, and sound and temperature by introducing functional units.[2] Thus, such supramolecular gels are considered as smart and versatile functional materials for applications in solar cells,[3] ion and molecular recognition,[4] light switches,[5] logic gates,[6] biomimetic systems,[7] and electronics.[8] Among various supramolecular gels, fluorescent organogels have attracted intense interest and are extensively studied because of their promising applications in optoelectronics and fluorescence sensors.

In this study, we designed and synthesized a series of 4-nitrophenylacrylonitrile and phenylacrylonitrile derivatives to obtain temperature-controlled fluorescent switches. Some derivatives with longer alkyl chains and nitro group could form gels in some organic solvents. However, phenylacrylonitrile derivatives without the nitro group were not gelator. This result suggests that the electron withdrawing nitro moiety is important for gel formation because the nitro group increases the molecular dipole moment and then enhances the intermolecular interaction, which was confirmed by the single crystal structure of **C4CNPA**. Interestingly, the organogels formed by **CnCNPA** could be used as fluorescent switches controlled by temperature because gels have stronger fluorescence relative to solutions.

Experimental Section

Instruments. Infrared spectra were measured using a Nicolet-360 FT-IR spectrometer by incorporating the samples in KBr disks. The UV-vis absorption spectra were determined on a Mapada UV-1800pc spectrophotometer. C, H, and N elemental analyses were performed on a Perkin-Elmer 240C elemental analyzer. Photoluminescence measurements were taken on a Shimadzu RF-5301 Luminescence Spectrometer. The fluorescence spectra of gels were measured in a 1mm cell by right angle observation. NMR spectra were carried out on Mercury plus 500 MHz. Mass spectra were obtained with Agilent 1100 MS series and AXIMA CFR MALDI-TOF (Compact) mass spectrometers. SEM images were carried out on a Japan Hitachi model X-650 Scan electron microscope. The samples for SEM observation were prepared by a method of drop-cast film. The samples were then kept overnight in a vacuum oven at room temperature followed by coating of gold. Small angle X-ray diffraction (XRD) patterns were obtained on a (λ=1.5418 Å), by employing a scanning rate of 0.02° s^{-1} in the 2θ from 1.1 to 10°.

The samples were prepared by casting the wet gels on glass slides and drying at room temperature. The fluorescence quantum yields (Φ) of **CnCNPA** in toluene were measured by comparing to a standard (9, 10-diphenylanthracene in benzene with a Φ of 0.85). The excitation wavelength was 390 nm. The optimal molecular configurations of **C1CNPA** and **C1CPA** were obtained by density functional theory (DFT) calculation at B3LYP/6-31G level with the Gaussian 09W program package.[9]

Single crystal was obtained in the toluene solution by slow solvent vaporization. Single crystal of **C4CNPA** was selected for X-ray diffraction analysis on in a Rigaku RAXIS-RAPID diffractometer using graphite-monochromated Mo-Kα radiation (λ = 0.71073 Å). The crystals were kept at room temperature during data collection. The structures were solved by the direct methods and refined on F2 by full-matrix least-square using the SHELXTL-97 program.[10] The C, N, O and H atoms were easily placed from the subsequent Fourier-difference maps and refined anisotropically. CCDC 993696 contains the supplementary crystallographic data for this paper.

Gelation Test. The solution containing weighed compound in organic solvent was heated in a sealed test tube with 1 cm diameter in an oil bath until the solid were dissolved. After the solution was allowed to stand at room temperature for 6 h, the state of the mixture was evaluated by the "stable to inversion of a test tube" method.

Synthetic procedures and characterizations. The synthesis route of compounds **CnCNPA** and **CnCPA** was shown in Scheme 1. 4-nitrophenylacetonitrile, **2a-c** and **3a-d** were synthesized by the procedures reported previously.[11]

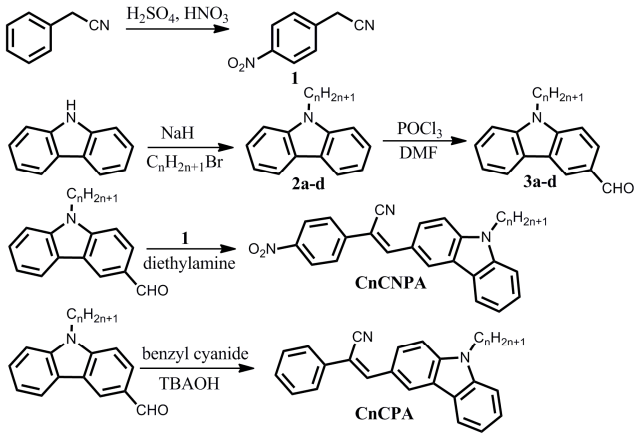

a = -$(CH_2)_3CH_3$; b = -$(CH_2)_7CH_3$; c = -$(CH_2)_{11}CH_3$; d = -$(CH_2)_{17}CH_3$

n=4, **C4CNPA**; n=8, **C9CNPA**; n=12, **C12CNPA**; n=16, **C16CNPA**
n=8, **C8CPA**; n=12, **C12CPA**; n=16, **C16CPA**

Scheme 1 Synthesis route of **CnCNPA** and **CnCPA**.

(Z)-3-(9-butylcarbazolyl)-2-(4-nitrophenyl)acrylonitrile (**C4CNPA**): **3a** (1.0 g, 4.0 mmol), 4-nitrophenylacetonitrile (0.84 g, 5.2 mmol) and ethanol (20 mL) was added into a 100 mL round-bottomed flask. After the solid was dissolved upon heating, 1 mL diethylamine was added and the mixture was refluxed for 10h. And then, the solution was cooled to room temperature. The product was obtained by vacuum suction filtration and washing by cooled ethanol. Yield: 88 %. mp: 216.5 ºC. Element analysis (%): calculated for $C_{25}H_{21}N_3O_2$: C, 75.93; H, 5.35; N, 10.63; Found: C, 76.11; H, 5.38; N, 10.59. ^{1}H NMR ($CDCl_3$, 500 MHz, ppm), δ = 8.68 (s, 1H), 8.27 (d, J = 8.6 Hz, 2H), 8.16 (t, J = 8.1 Hz, 2H), 7.87-7.78 (m, 3H), 7.53 (t, J = 7.6 Hz, 1H), 7.47 (d, J = 8.5 Hz, 1H) , 7.45 (d, J =8.0 Hz, 1H), 7.31 (t, J = 7.4 Hz, 1H), 4.33 (t, J = 7.2 Hz, 2H), 1.93-1.79 (m, 2H), 1.43-1.33 (m, 2H), 0.97 (t, J = 7.3 Hz, 3H). MS (MALDI-TOF), m/z: cal: 395.16, found: 395.10.

(Z)-3-(9-octylcarbazolyl)-2-(4-nitrophenyl)acrylonitrile (**C8CNPA**): By following the synthetic procedure for **C4CNPA**, **C8CNPA** was synthesized with compound **3b** (1.7 g, 5.6 mmol), 4-nitrophenylacetonitrile (1.0 g, 6.2 mmol), and diethylamine (1 mL). Yield: 85 %. mp: 158.5 ºC. Element analysis (%): calculated for $C_{29}H_{29}N_3O_2$: C, 77.13; H, 6.47; N, 9.31; Found: C, 77.16; H; 6.43; N, 9.39. ^{1}H NMR ($CDCl_3$, 500MHz, ppm), δ = 8.71 (d, J = 2.0 Hz, 1H), 8.31 (t, J = 8.6 Hz, 2H), 8.18 (t, J = 8.1 Hz, 2H), 7.88-7.86 (m, 3H), 7.53 (t, J = 7.6 Hz, 1H), 7.49 (d,J = 8.5 Hz, 1H), 7.46 (d, J =8.0 Hz, 1H), 7.32 (t, J = 7.4 Hz, 1H), 4.34 (t, J = 7.0 Hz, 2H), 1.93-1.88 (m, 2H), 1.33-1.23 (m, 10H), 0.87 (t, J = 7.0 Hz, 3H). MS (MALDI-TOF), m/z: cal: 451.23, found: 451.20.

(Z)-3-(9-dodecylcarbazolyl)-2-(4-nitrophenyl)acrylonitrile (**C12CNPA**): By following the synthetic procedure for **C4CNPA**. Yield: 84 %. mp: 131.5 ºC. Element analysis (%): calculated for $C_{33}H_{37}N_3O_2$: C, 78.07; H, 7.35; N, 8.28; Found: C, 78.05; H, 7.30; N, 8.23. ^{1}H NMR ($CDCl_3$, 500 MHz, ppm), δ = 8.70 (s, 1H), 8.30 (d, J = 8.7 Hz, 2H), 8.23 – 8.11 (m, 2H), 7.86 (d, J = 8.9 Hz, 3H), 7.53 (t, J = 7.6 Hz, 1H), 7.48 (d, J = 8.7 Hz, 1H), 7.45 (d, J = 8.2 Hz, 1H), 7.32 (t, J = 7.4 Hz, 1H), 4.33 (t, J = 7.2 Hz, 2H), 1.95 – 1.82 (m, 2H), 1.42–1.20 (m, 18H), 0.87 (t, J = 6.8 Hz, 3H). MS (MALDI-TOF), m/z: cal: 507.29, found: 507.23.

(Z)-3-(9-hexadecylcarbazolyl)-2-(4-nitrophenyl)acrylonitrile (**C16CNPA**): By following the synthetic procedure for **C4CNPA**. Yield: 86 %. mp: 81.0 ºC. Element analysis (%): calculated for $C_{37}H_{45}N_3O_2$: C, 78.83; H, 8.05; N, 7.45; Found: C, 78.75; H, 8.00; N, 7.48. ^{1}H NMR ($CDCl_3$, 500 MHz, ppm) δ = 8.74 (d, J = 1.6 Hz, 1H), 8.37 – 8.31 (m, 2H), 8.22 (dd, J = 8.7, 1.7 Hz, 1H), 8.19 (d, J = 7.8 Hz, 1H), 7.93 – 7.87 (m, 3H), 7.56 (t, J = 7.2 Hz, 1H), 7.52 (d, J = 8.7 Hz, 1H), 7.49 (d, J = 8.2 Hz, 1H), 7.35 (t, J = 7.5 Hz, 1H), 4.37 (t, J = 7.3 Hz, 2H), 1.97 – 1.90 (m, 2H), 1.46 – 1.23 (m, 26H), 0.90 (t, J = 7.0 Hz, 3H). MS (MALDI-TOF), m/z: cal: 563.35, found: 563.30.

(Z)-3-(9-octylcarbazolyl)-2-Phenyl-acrylonitrile (**C8CPA**): After **3b** (1.2 g, 3.9 mmol) and phenylacetonitrile (0.49 mL, 4.3 mmol) in ethanol was dissolved upon heating, 0.2 mL tetrabutylammonium hydroxide (TBAOH, 40% in water) was added and the mixture was refluxed for 10h. And then, the solution was cooled to room temperature. The product was obtained by vacuum suction filtration and washing by cooled ethanol. Yield: 85%. mp: Element analysis (%): calculated for $C_{29}H_{30}N_2$: C, 85.67; H, 7.44; N, 6.89; Found: C, 85.69; H, 7.41; N, 6.86. ^{1}H NMR ($CDCl_3$, 500MHz, ppm), δ = 8.64 (d, J = 1.7 Hz, 1H), 8.15 (dd, J = 13.3, 4.7 Hz, 2H), 7.72 (dd, J = 5.4, 3.2 Hz, 3H), 7.54 – 7.49 (m, 1H), 7.47 (d, J = 7.0 Hz, 2H), 7.46 – 7.42 (m, 2H), 7.37 (t, J = 7.4 Hz, 1H), 7.29 (dd, J = 11.3, 4.3 Hz, 1H), 4.32 (t, J = 7.3 Hz, 2H), 1.89 (m, 2H), 1.43 – 1.20 (m, 10H), 0.89 – 0.81 (t, J = 7.0 Hz, 3H). MS (MALDI-TOF), m/z: cal: 406.24, found: 406.25.

(Z)-3-(9-dodecylcarbazolyl)-2–Phenyl-acrylonitrile (**C12CPA**): By following the synthetic procedure for **C8CPA**.

Yield: 86 %. Element analysis (%): calculated for $C_{33}H_{37}N_2$: C, 78.07; H, 7.35; N, 8.28; Found: C, 78.03; H, 7.21; N, 8.22. ^{1}H NMR ($CDCl_3$, 500 MHz, ppm), δ = 8.65 (d, J = 1.3 Hz, 1H), 8.15 (dd, J = 13.7, 4.8 Hz, 2H), 7.75 – 7.69 (m, 3H), 7.51 (t, J = 7.2 Hz, 1H), 7.47 (d, J = 6.3 Hz, 2H), 7.45 (dd, J = 10.6, 5.0 Hz, 3H), 7.37 (t, J = 7.4 Hz, 1H), 7.29 (t, J = 7.3 Hz, 1H), 4.32 (t, J = 7.2 Hz, 2H), 1.94 – 1.84 (m, 2H), 1.43 – 1.20 (m, 18H), 0.87 (t, J = 7.0 Hz, 3H). MS (MALDI-TOF), m/z: cal: 462.30, found: 462.31.

(Z)-3-(9-hexadecylcarbazolyl)-2-Phenyl-acrylonitrile (C16CPA): By following the synthetic procedure for **C8CPA**. Yield: 83 %. Element analysis (%): calculated for $C_{37}H_{45}N_2$: C, 85.66; H, 8.94; N,5.40; Found: C, 85.63; H, 8.89; N, 5.43. ^{1}H NMR ($CDCl_3$, 500MHz, ppm), δ = 8.64 (d, J = 1.3 Hz, 1H), 8.19 – 8.12 (m, 2H), 7.74 – 7.69 (m, 3H), 7.51 (t, J = 7.7 Hz, 1H), 7.48 – 7.46 (m, 2H), 7.44 (t, J = 6.0 Hz, 2H), 7.37 (t, J = 7.3 Hz, 1H), 7.29 (t, J = 7.3 Hz, 1H), 4.32 (t, J = 7.3 Hz, 2H), 1.93–1.88 (m, 2H), 1.44–1.21 (m, 26H), 0.88 (t, J = 6.9 Hz, 3H). MS (MALDI-TOF), m/z: cal: 518.37, found: 518.30.

Results and discusion

Synthesis

Scheme 1 shows the synthesis routes of **CnCNPA** and **CnCPA**. Compound **1** was obtained through the nitration reaction of benzyl cyanide in a mixed acid. **3a-d** could be obtained by the Vilsmeier reaction of corresponding **2a-d** with DMF in the presence of $POCl_3$. **CnCNPA** and **CnCPA** were synthesized by a simple Knoevenagel reaction in the presence of different catalysts. The stronger acidity of methylene moiety in compound **1** needs a weak base (diethylamine) as a catalyst, but TBAOH as a strong base is necessary for benzyl cyanide because of its weak activity. The products were characterized by ^{1}H NMR spectroscopy, MALDI-TOF mass spectrometry, and C, H, N elemental analyses.

Gelation ability in organic solvents

Through the standard heating-and-cooling method,[12] the gelation abilities of **CnCNPA** and **CnCPA** were investigated. We found that the gelation properties were strongly affected by the nitro group and alkyl chain. For example, **CnCNPA** with C8, C12, and C16 alky chains could form gels in DMSO and some alcohol. However, the **CnCPA** solutions in these solvents remained in a solution state, or the precipitate was separated from the solutions. Although two types of compounds had large solubility and maintained the solution state in some solvents, such as CH_2Cl_2, $CHCl_3$, THF, benzene, and DMF, the solubility of **CnCPA** and **CnCNPA** were different in n-hexane, cyclohexane, acetone, ethyl acetate, and *n*-butanol. **CnCNPA** with nitro unit had lower solubility in these solvents. These results suggest that nitro moiety is very important for compounds to form gels in organic solvents.[13] The gelation ability of **CnCNPA** in the given solvents is relative to the length of the alkyl chain.[14] **C4CNPA** is not the gelator for selected solvents. Only **C8CNPA** could gelatinize acetone and ethyl acetate at high concentration, whereas **C12CNPA** and **C16CNPA** separated as depositions from their solutions in two solvents. **C12CNPA** is formed alone in n-butanol and t-Amyl alcohol. The minimal gelation concentration of **C8CNPA** in gelation solvents except in ethanol was generally lower compared with **C12CNPA** and **C16CNPA**.

Table 1 Gelation properties in different organic solvents.[a]

Solvent	C4CNPA	C8CNPA	C12CNPA	C16CNPA	C8CPA	C12CPA	C16CPA
Chloroform	S	S	S	S	S	S	S
Cyclohexane	I	I	P	P	S	S	S
Dichloromethane	S	S	S	S	S	S	S
n-Haxane	I	I	P	P	P	S	S
Petroleum ether	I	I	I	P	P	S	S
THF	S	S	S	S	S	S	S
Acetone	P	G (18)[b]	P	P	S	S	S
Ethyl acetate	P	G (18)	P	P	S	S	S
Toluene	S	S	S	S	S	S	S
o-Dichlorobenzene	S	S	S	S	S	S	S
DMF	S	S	S	S	S	S	S
DMSO	P	G (10)	G (4.1)	G (4.7)	S	S	P
Methanol	P	G (1.2)	G (2.5)	G (5.4)	P	P	P
Ethanol	P	G (2.0)	G (1.8)	G(7.1)	P	S	P
n-Butanol	P	P	G (8.8)	P	S	S	S
t-Amyl alcohol	P	P	G (6.7)	P	S	S	S
Tert-butanol	P	G (7.9)	P	G (10)	P	P	S

[a] G : stable gel formed at room temperature; S: soluble; I: insoluble; P: precipitate. [b] Minimal gelation concentration (MGC, mM).

Photophysical properties in solution

Becasue only **CnCNPA** could form gels in measured solvents, their spectral characteristics rather than those of **CnCPA** in solutions were studied. We found that **CnCNPA** with different alkyl chains had the same spectral behavior, so the **C8CNPA** was selected to show the spectral characteristic in solution. As shown in Fig. 1a, **C8CNPA** has an absorption band with a maximum of 404 nm in cyclohexane, which red-shifted to 408 nm in toluene, to 411 nm in THF and CH_2Cl_2, to 413 nm in $CHCl_3$, and to 421 in DMF. The red-shifted absorption peaks in polar solvents suggest that **C8CNPA** has a larger dipole moment in the excited state than in the ground state,[15] which can be confirmed by solvent-dependent fluorescence spectra. An emission peak at 449 nm for **C8CNPA** in cyclohexane was found (Fig. 1b), which indicates a Stockes shift of 2480 cm^{-1}. In THF, the emission peak located at 542 nm, implying green fluorescence and a Stockes shift of 5881 cm^{-1}. With the further increase in the solvent polarity, the fluorescence exhibited a continued red shift, whereas the emission color changed to yellow, orange, and red in $CHCl_3$, CH_2Cl_2 and DMF, respectively.[16] The largest Stockes shift was observed in DMF (7386 cm^{-1}). Such significant red-shift of emission band in polar solvents indicates an intramolecular charge-transfer (ICT) characteristic for the excited state.[17] A linear relationship between the emission maximum energy and

the Lippert solvent polarity instead of cyclohexane was found (Fig. 1c), and the emission band in cyclohexane was narrow and had a shoulder peak. It indicates that the emission in cyclohexane is the locally excited one and fluorescence in other solvents is attributed to ICT emission.[18] Therefore, **C8CNPA** is a typical D-π-A molecule.

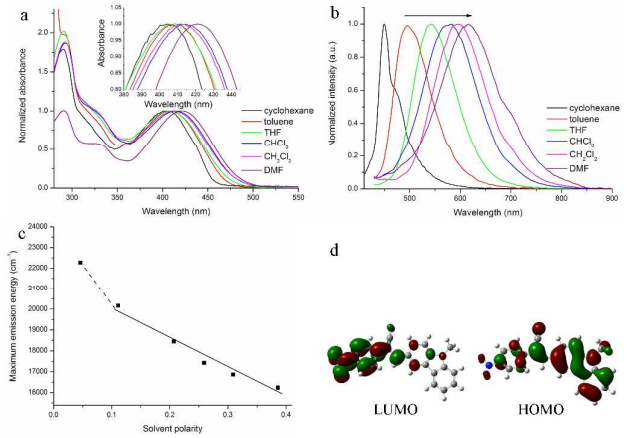

Fig. 1 Normalized absorption (a) and emission (b) spectra of **C8CNPA** in different solvents (1×10^{-6} M). λ_{ex} = 390 nm. Lippert–Mataga plot: fluorescence emission maximum energy of **C8CNPA** as a function of solvent polarity. (d) Frontier orbital plots of the HOMO and LUMO of **C1CNPA**. The long alkyl chain was replaced by the methyl group to simplify the calculation.

Quantum chemical calculations were performed on **C1CNPA** by density functional theory calculations at the B3LYP/6-31G(d) level to further clarify the ICT transition. Fig. 1d shows that the HOMO state density is distributed at the 4-nitrobenzene and vinyl units. By contrast, the LUMO density is mainly localized on the carbazole and vinyl moieties. The stimulated absorption spectrum of **C1CNPA** shows an absorption peak at ca. 451 nm (Fig. S1) ascribing to the HOMO→LUMO transition. Therefore, light excitation clearly induces a charge distribution change from donor to acceptor. This result further proves that the maximum absorption and emission are due to the ICT transition.[19] We also obtained the optimal conformation of **C1CPA** and compared their dipole moments to understand the role of the nitro unit on gel formation (Fig. S2). The result suggests that the dipole moment of **C1CNPA** (10.6269 Debye) is larger than that of **C1CPA** (4.3811 Debye), implying that the larger dipole moment may be responsible for the gel formation.[20]

We also found that **C8CNPA** was a weak emissive fluorophore. The fluorescence quantum yield (Φ) in toluene was as low as 0.21 %. In other solvents, the Φs were also lower than 1%. Φs of **C4CNPA**, **C12CNPA** and **C16CNPA** in toluene were 0.21%, 0.25%, and 0.25%, respectively. Thus, small Φs are ascribed to the intramolecular rotation of a single bond and the existence of cyano moiety, which induces the twisted conformation in the isolated state because of the steric interaction between the bulky cyano unit and the neighboring hydrogen atoms.[21] This condition could be confirmed by the optimal geometry of **C1CNPA** (Fig. S2a), in which the dihedral angles of the vinyl group with carbazole and 4-nitrobenzene units are 5.8° and 24.4°.

Self-assembly in gel state

First, the morphologies of the gelators in gel phases were observed and compared. Fig. 2 shows the scanning electron microscope (SEM) images of **C8CNPA**, **C12CNPA**, and **C16CNPA** in ethanol and DMSO. Three compounds had similar morphologies in DMSO gels and self-assembled into a one-dimensional (1D) nanoribbon with a large aspect ratio (Figs. 2b, 2d, and 2f). However, the self-assemblies in ethanol gels were different. Larger ribbons with larger widths were observed for **C8CNPA** (Fig. 2a). Some ribbons were more than 10 μm in width. **C12CNPA** and **C16CNPA** could form thinner and longer ribbons in ethanol gels, whereas right-handed and left-handed twisted ribbons were found in **C16CNPA** ethanol gel. Because longer alkyl chain will increase the disordering of molecular packing, so gelator with long chain can self-assemble into thin and soft fiber.[22] This result suggests that the length of the alkyl chain strongly affect the gelator morphologies in solvents.

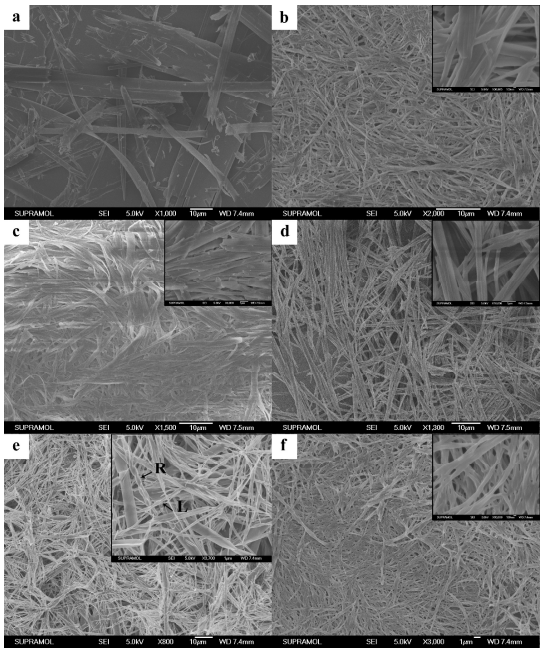

Fig. 2 SEM images of **C8CNPA** (a, b), **C12CNPA** (c, d) and **C16CNPA** (e, f) gels in ethanol and DMSO. Insets are the enlarged images.

When the yellow sols of **C8CNPA** in ethanol and DMSO were cooled to room temperature and transferred into turid gels (Fig. S3), the system color changed into orange, suggesting the existence of π-π interaction between aromatic units. Therefore, the absorption spectrum was used to monitor this process. As shown in Fig. 3, when the hot sols in the two solvents were cooled, the absorption peaks started firstly to increase and slightly red-shifted because of the increase in the π-conjugation degree in low temperature. After 1 min, the absorption peaks gradually decreased and further shifted to a longer wavelength region. Weak absorption bands at approximately 500 nm appeared and gradually heightened, which explains orange color of gels. Temparature-dependent absorption spectra in two solvents showed similar spectral change (Fig. S4). There is a red-shift of 4 nm during gelation in ethanol, and a red-shift of 2 nm in DMSO. In addition, the dilute solutions of **C8CNPA** in two solvents had blue-shifted absorption bands (9 nm and 3 nm in

ethanol and DMSO, respectively) relative to those of gels (Fig. S5). These spectral changes illustrate the *J*-aggregate formation during gelation.[23] The absorption spectra of **C12CNPA** and **C16CNPA** during the gel process were also measured. As shown in Fig. S6, maximal absorption peaks for **C12CNPA** and **C16CNPA** had blue-shifts of 7 nm and 10 nm relative to those of hot sols. Moreover, the gels in ethanol possessed blue-shifted absorption bands relative to those of dilute solutions (Fig. S7). This observation suggests that the packing models of **C12CNPA** and **C16CNPA** in gels are different from that of **C8CNPA**, although the absorption band at 500 nm also appeared in their gels. In the **C12CNPA** and **C16CNPA** gels, the *H*-aggregate formation is responsible for the blue-shifted absorption. [24]

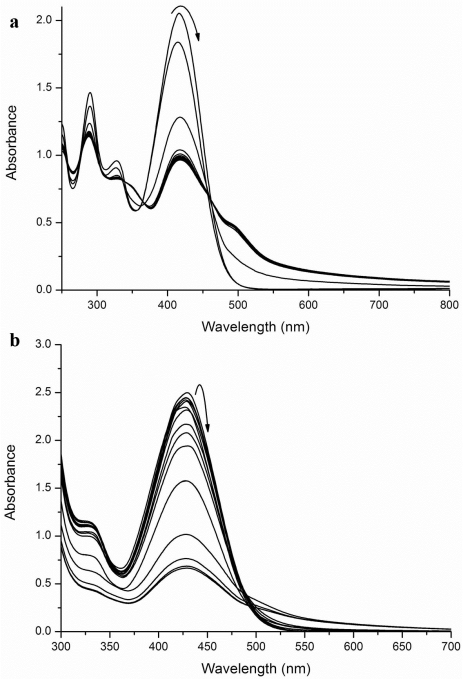

Fig. 3 Absorption spectra of **C8CNPA** in ethanol and DMSO during gelation, C = 3.2 mM in ethanol, and 19 mM in DMSO. The interval time is 1 min.

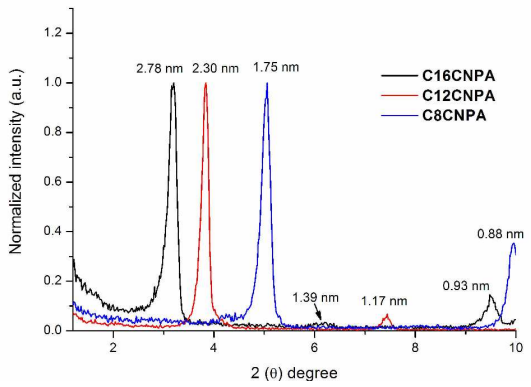

Fig. 4 XRD patterns of **C8CNPA**, **C12CNPA,** and **C16CNPA** xerogels from ethanol.

Considering that X-ray diffraction (XRD) always shows the stack model of gelator in gels, small-angle XRD patterns of the three gelators in ethanol gels were investigated (Fig. 4). **C8CNPA**, **C12CNPA**, and **C16CNPA** clearly adopts a lamellar packing structure with packing periods evaluated to be 1.75, 2.30, and 2.78 nm, respectively.[25] The XRD patterns of the DMSO xerogels were also obtained. **C8CNPA** and **C16CNPA** DMSO xerogels possessed similar lamellar structures and stacking periods to corresponding ethanol xerogels (Fig. S8). However, two types of layer period in the DMSO xerogel of **C12CNPA** were observed. One layer was similar to that of ethanol xerogel, whereas another one had a longer period of 2.13 nm, indicating that two types of molecular packing models. These results show that three gelators self-assembled into ribbons with a layer packing structure in gel phases.

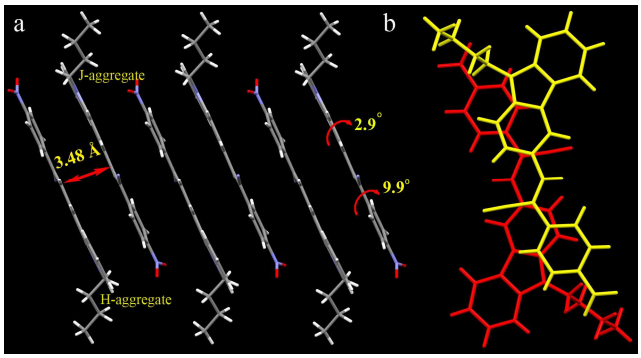

Fig. 5 (a) 1D packing of **C4CNPA** in crystal, and (b) top view of one dimer.

We attempted to obtain single crystals of three gelators to further understand the detailed stacking model in gels. However, only thin and longer orange fibers were grown from their solutions. Fortunately, enough large orange single crystals of **C4CNPA** from toluene solution were obtained, and its single-crystal structure and crystal data are shown in Fig. 5 and Table S1. In the crystal, the dihedral angles between the vinyl and two benzene rings were very small at 2.9° and 9.9°, respectively, indicating that the planarity of the molecule is good. The molecules were also arranged into 1D stacking, in which one anti-parallel dimer appeared repeatedly. Molecules adopt anti-parallel packing rather than parallel ones in crystal because of the inherent large dipole moment of **C4CNPA**. Anti-parallel stacking permits sufficient electrostatic attraction force between molecules. The distance between two molecules in the dimer was 3.48 Å, suggesting a strong intermolecular interaction between molecules. We found a new peak at 500 nm and a blue-shifted absorption band at 383 nm in the absorption spectrum of the crystal (Fig. S9) relative to its solution. The crystal absorption spectrum could be explained by the crystal structure. Two molecules in the dimer were stacked together face-to-face, producing an H-aggregate and then inducing blue-shifted absorption peak. The sliding angle between the two dimers is larger than that in the dimer itself, so a red-shifted absorption band appears that indicates a J-aggregate (Fig. 5a). This spectral change is similar to those in **C12CNPA** and **C16CNPA** gels, so **C12CNPA** and **C16CNPA** in gels have similar intermolecular packing models (Fig. 6).

Considering that **C8CNPA** had red-shifted absorption during gelation, a large dipole moment, and the existence of an absorption peak at 500 nm, **C8CNPA** reasonably stacked together in the anti-parallel model. A different dimer structure from **C4CNPA** also exists. As shown in Fig. 6, the sliding angles between two molecules in the dimer and between two dimers are

large enough to induce two red-shifted absorption bands. The difference of van der Waals interaction between alkyl chains should be in charge of different molecular stacking in gels because aromatic moieties of three compounds are same, and the length of alkyl chain is only different.

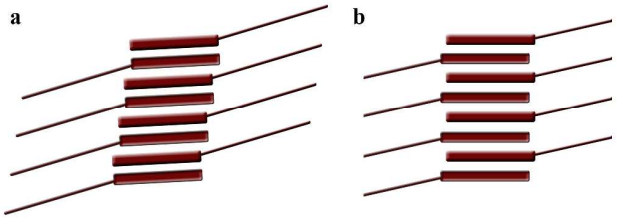

Fig. 6 Packing models in gels for (a) **C12CNPA** and **C16CNPA**, and for (b) **C8CNPA**.

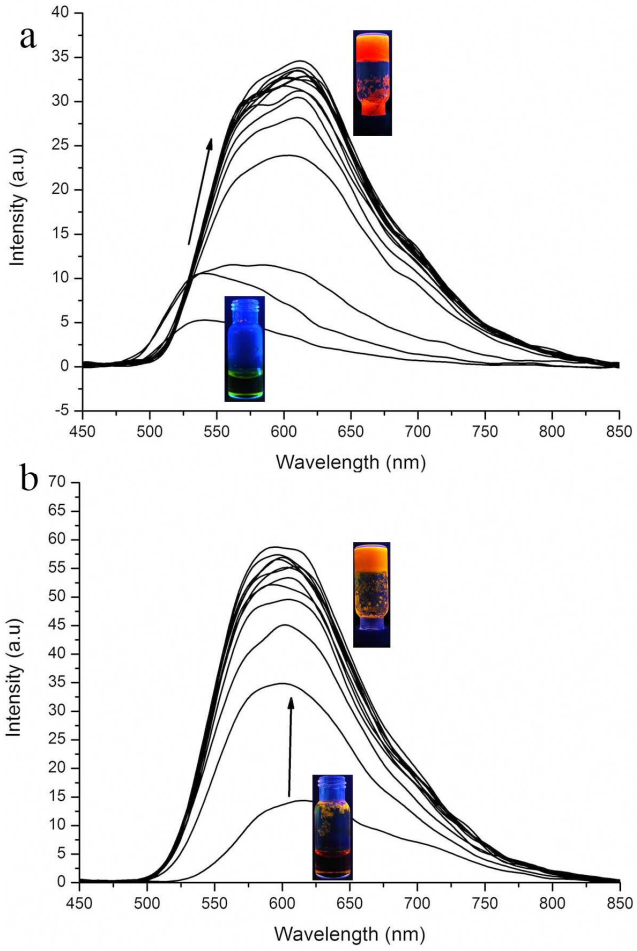

Fig. 7 Fluorescence spectra of **C8CNPA** in (a) ethanol and (b) DMSO during gelation. C = 3.2 mM in ethanol, 19 mM in DMSO, and λ_{ex} = 410 nm. The interval time is 1 min. Insets are photos of **C8CNPA** in ethanol and DMSO under 365 nm light.

Gelation-induced emission enhancement

Based on the above discussions, **CnCNPA** is known to exhibit weak emission and small Φs in solution because of the existence of cyano moiety and free intramolecular rotation. We also found that the hot sols of the three gelators in ethanol and DMSO emitted weak fluorescence, but stronger emission for corresponding gels was observed. Thus, our gels exhibited gelation-induced emission enhancement. Given that high temperature always quenches fluorophore emission, we selected the hot DMSO sol (100 °C) of **C8CNPA** at a low concentration of 40 mM, which needs 30 min to form a gel. When the sol changed into a gel, the sol had been cooled to room temperature. The fluorescence of the sol was very weak before gelation. When the sol started to become turbid and form a gel, the emission intensity of system increased swiftly. This result suggests that the emission enhancement originated from the molecular aggregate.[26]

Fig. 7 shows the fluorescence spectral change for **C8CNPA** in ethanol and DMSO during gelation. The hot ethanol sol of **C8CNPA** emitted weak green fluorescence with a maximum of 539 nm. After 2 min, the emission band at approximately 600 nm appeared and gradually enhanced. After 15 min, the system changed into a gel and had an orange red emission with more than 6-fold intensity compared with the sol. In DMSO, the system also exhibited similar emission enhancement during gel formation. Weak and red fluorescence for the hot DMSO sol was observed, but the corresponding gel emitted blue-shifted orange fluorescence with a maximum at 594 nm and 4-fold increase in the emission intensity. Temperature-dependent fluorescence spectra showed the same result (Fig. S10). At low temperature the system had strong emission, and fluorescence intensity decrease at higher temperature. Through comparison of the optimal configuration from theory calculation and molecular structure in crystal state, the enhanced emission of the gel is attributed to the synergetic effect of the restricted molecular motion and the formation of more coplanar conformations.[27] In addition, the similar emission wavelengths of gels in ethanol and DMSO should attribute to the same molecular stacking in two solvents.

As shown above, the gels with enhanced emission were obtained when the hot sols were cooled. Therefore, when the gels were heated to form the sol, the obvious fluorescent change was anticipated. As expected, when the temperature was higher than the sol-gel phase transition temperatures (T_{gel}s) of gels and gels transferred into sols, the emission intensity sharply decreased, showing temperature-controlled fluorescence switches. Given that T_{gel}s could simply be adjusted by the gelator concentration, the sensing temperatures of these switches could also be decided by gelator concentration. As shown in Fig. S6, the T_{gel} values rise nonlinearly with the increasing gelator concentration. For example, the **C8CNPA** gel (11 mM) changed into a sol at 45 °C, accompanied by fluorescence decrease. As the concentration increased to 16 mM and 22 mM, the T_{gel} also increased to 59 °C and 70 °C, respectively. The solvent is also important for the fluorescent color change. In ethanol, the fluorescence color changed from orange red to green, whereas the DMSO gel with stronger orange emission transformed into a red solution with weak red fluorescence.

Conclusion

A series of 4-nitrophenylacrylonitrile and phenylacrylonitrile derivatives consisting of carbazole moiety was synthesized. Some of these derivatives with longer alkyl chains and nitro group

could gelatinize some organic solvents. However, phenylacrylonitrile derivatives were not gelators. This result suggests that the electron withdrawing nitro moiety is important for gel formation because it makes molecules with large dipole moments, which was proven by theory calculation and the single-crystal structure. The single crystal structure of **C4CNPA** implies that gelators might adopt an anti-parallel molecular stacking given the larger ground-state dipole moment. The organogels also exhibited enhanced fluorescence relative to solutions. This result indicates that the gels can be used as temperature-sensitized fluorescent switches. The switch temperature can be easily adjusted by gelator concentration.

Acknowledgements

This work was financially supported by the National Natural Science Foundation of China (21103067, 21374041, and 51102081), the Youth Science Foundation of Jilin Province (20130522134JH), the Science and Technology Development Plan of Jilin Province, China (20130521003JH), the Open Project of the State Key Laboratory of Supramolecular Structure and Materials (SKLSSM201203), the Open Project of State Key Laboratory of Theoretical and Computational Chemistry (K2013-02).

Notes and references

[a] *State Key Laboratory of Supramolecular Structure and Materials, College of Chemistry, Jilin University, Changchun, P. R. China, E-mail: xuepengchong@jlu.edu.cn; luran@mail.jlu.edu.cn*
[b] *College of Chemistry, Beijing Normal University, Beijing, 100875, P. R. China*
[c] *College of Chemistry, Jilin University, Changchun, P. R. China*
[d] *Key Laboratory of Functional Inorganic Material Chemistry (MOE), School of Chemistry and Materials Science, Heilongjiang University, Harbin, P. R. China*

† Electronic Supplementary Information (ESI) available: [Calculated absorption spectrum and optimal structure, Photos of gels, the absorption spectra of three gelators in solution and gels, the absorption sepctra of **C4CNPA** in solution and crystal, XRD patterns of DMSO gels, crystal data of **C4CNPA**, plots of T_{gel}s vs concentration, and CCDC 993696]. See DOI: 10.1039/b000000x/

1 A. Nelson, *Nat. Mater.*, 2008, **7**, 523; P. Theato, B. S. Sumerlin, R. K. O'Reilly and T. H. Epps, III, *Chem. Soc. Rev.*, 2013, **42**, 7055-7056; H. Shao, C. Wang, J. Zhang and S. Chen, *Macromolecules*, 2014, **47**, 1875-1881; X. Zhang, Z. Chi, Y. Zhang, S. Liu and J. Xu, *J. Mater. Chem. C*, 2013, **1**, 3376-3390; L. Sun, W. M. Huang, Z. Ding, Y. Zhao, C. C. Wang, H. Purnawali and C. Tang, *Mater. Design*, 2012, **33**, 577-640; H. Kuroki, I. Tokarev, D. Nykypanchuk, E. Zhulina and S. Minko, *Adv. Funct. Mater.*, 2013, **23**, 4593-4600.

2 P. Terech and R. G. Weiss, *Chem. Rev.*, 1997, **97**, 3133-3359; b) J. H. van Esch and B. L. Feringa, *Angew. Chem. Int. Ed.*, 2000, **39**, 2263-2266; X. Yu, X. Cao, L. Chen, H. Lan, B. Liu and T. Yi, *Soft Matter*, 2012, **8**, 3329-3334; R. J. Kumar, J. M. MacDonald, T. B. Singh, L. J. Waddington and A. B. Holmes, *J. Am. Chem. Soc.*, 2011, **133**, 8564-8573; L. Zhang, C. Liu, Q. Jin, X. Zhu and M. Liu, *Soft Matter*, 2013, **9**, 7966-7973; G. Zhao, L. Chen, W. Wang, J. Zhang, G. Yang, D. Wang, Y. Yu and H. Yang, *Chem. Eur. J.*, 2013, **19**, 10094-10100; P. Mukhopadhyay, N. Fujita, A. Takada, T. Kishida, M. Shirakawa and S. Shinkai, *Angew. Chem. Int. Ed.*, 2010, **49**, 6338-6342; H. Peng, L. Ding, T. Liu, X. Chen, L. Li, S. Yin and Y. Fang, *Chem.–Asian J.*, 2012, **7**, 1576-1582; Z. Zhao, J. W. Y. Lam and B. Z. Tang, *Soft Matter*, 2013, **9**, 4564-4579; Z. Sun, Z. Li, Y. He, R. Shen, L. Deng, M. Yang, Y. Liang and Y. Zhang, *J. Am. Chem. Soc.*, 2013, **135**, 13379-13386; A. Dawn, T. Shiraki, H. Ichikawa, A. Takada, Y. Takahashi, Y. Tsuchiya, L. T. N. Lien and S. Shinkai, *J. Am. Chem.Soc.* 2012, **134**, 2161-2171; S. K. Samanta and S. Bhattacharya, *Chem. Commun.*, 2013, **49**, 1425-1427; S. Bhattacharya and S. K. Samanta, *Langmuir*, 2009, **25**, 8378–8381.

3 I. D. Tevis, W. Tsai, L. C. Palmer, T. Aytun and S. I. Stupp, *ACS Nano*, 2012, **6**, 2023-2040; P. Xue, Q. Xu, P. Gong, C. Qian, Z. Zhang, J. Jia, X. Zhao, R. Lu, A. Ren and T. Zhang, *RSC Adv.*, 2013, **3**, 26403-26411; Z. Yu, D. Qin, Y. Zhang, H. Sun, Y. Luo, Q. Meng and D. Li, Energy Environ. Sci., 2011, **4**, 1298-1305; S. Park, I. Y. Song, J. Lim, Y. S. Kwon, J. Choi, S. Song, J. Lee and T. Park, Energy Environ. Sci., 2013, **6**, 1559-1564.

4 Q. Jin, L. Zhang, X. Zhu, P. Duan and M. Liu, *Chem. Eur. J.*, 2012, **18**, 4916-4922; X. Wang, P. Duan and M. Liu, *Chem. Asian J.*, 2014, **9**, 770-778; H. Jintoku, M. Takafuji, R. Oda and H. Ihara, *Chem. Commun.*, 2012, **48**, 4881-4483; W. Miao, L. Zhang, X. Wang, L. Qin and M. Liu, *Langmuir*, 2013, **29**, 5435-5442.

5 X. Cao, A. Gao, H. Lv, Y. Wu, X. Wang and Y. Fan, *Org. Biomol. Chem.*, 2013, **11**, 7931-7937; P. Xue, Ran Lu, G. Chen, Y. Zhang, H. Nomoto, M. Takafuji and H. Ihara, *Chem. Eur. J.*, 2007, **13**, 8231-8239; J. T. van Herpt, J. Areephong, M. C. A. Stuart, W. R. Browne and B. L. Feringa, *Chem. Eur. J.*, 2014, **20**, 1737-1742; S. Bhattacharjee, S. Datta and S. Bhattacharya, *Chem. Eur. J.*, 2013, **19**, 16672-16681.

6 P. Xue, R. Lu, J. Jia, M. Takafuji and H. Ihara, *Chem. Eur. J.*, 2012, **18**, 3549-3558; J.W. Chung, S. Yoon, S. Lim, B. An and S.Y. Park, *Angew. Chem. Int. Ed.*, 2009, **48**, 7030-7034.

7 C. Feng, X. Dou, D. Zhang and H. Schönherr, Macromol. Rapid Commun., 2012, **33**, 1535-1541; J. Zhou , X. Du , Y. Gao , J. Shi and Bing Xu, *J. Am. Chem. Soc.*, 2014, **136**, 2970-2973.

8 J. P. Hong, M. C. Um, S. R. Nam, J. I. Hong and S. Lee, *Chem. Commun.*, 2009, 310-312; W.-W. Tsai, I. D. Tevis, A. S. Tayi, H. Cui and S. I. Stupp, *J. Phys. Chem. B*, 2010, **114**, 14778-14786; D. A. Stone, A. S. Tayi, J. E. Goldberger, L. C. Palmera and S. I. Stupp, *Chem. Commun.*, 2011, **47**, 5702-5704; X. Yang, G. Zhang, D. Zhang, J. Xiang, G. Yang and D. Zhu, *Soft Matter*, 2011, **7**, 3592-3598; S. Prasanthkumar, A. Saeki, S. Seki and A. Ajayaghosh, *J. Am. Chem. Soc.*, 2010, **132**, 8866-8867; S. Prasanthkumar, A. Gopal and A. Ajayaghosh, *J. Am. Chem. Soc.*; 2010, **132**, 13206-13207; D. B. Amabilino and J. Puigmartí-Luis, *Soft Matter*, 2010, **6**, 1605-1612; S. Datta and S. Bhattacharya, *Chem. Commun.*, 2012, **48**, 877–879.

9 Gaussian 09, Revision A.02, M. J. Frisch, G. W. Trucks, H. B. Schlegel, G. E. Scuseria, M. A. Robb, J. R. Cheeseman, G. Scalmani, V. Barone, B. Mennucci, G. A. Petersson, H. Nakatsuji, M. Caricato, X. Li, H. P. Hratchian, A. F. Izmaylov, J. Bloino, G. Zheng, J. L. Sonnenberg, M. Hada, M. Ehara, K. Toyota, R. Fukuda, J. Hasegawa, M. Ishida, T. Nakajima, Y. Honda, O. Kitao, H. Nakai, T. Vreven, J. A. Montgomery, Jr., J. E. Peralta, F. Ogliaro, M. Bearpark, J. J. Heyd, E. Brothers, K. N. Kudin, V. N. Staroverov, R. Kobayashi, J. Normand, K. Raghavachari, A. Rendell, J. C. Burant, S. S. Iyengar, J. Tomasi, M. Cossi, N. Rega, J. M. Millam, M. Klene, J. E. Knox, J. B. Cross, V. Bakken, C. Adamo, J. Jaramillo, R. Gomperts, R. E. Stratmann, O. Yazyev, A. J. Austin, R. Cammi, C. Pomelli, J. W. Ochterski, R. L. Martin, K. Morokuma, V. G. Zakrzewski, G. A. Voth, P. Salvador, J. J. Dannenberg, S. Dapprich, A. D. Daniels, Ö. Farkas, J. B. Foresman, J. V. Ortiz, J. Cioslowski, and D. J. Fox, Gaussian, Inc., Wallingford CT, 2009.

10 G. M. Sheldrick, SHELXL-97. Program Crystal Structure Refinement. University of Göttingen, Germany, 1997.

11 Y. Zhan, K. Cao, C. Wang, J. Jia, P. Xue, X. Liu, X. Duan and R. Lu, *Org. Biomol. Chem.*, 2012, **10**, 8701-8709; Y. Zhan, K. Cao, P. Xue and R. Lu, *Tetrahedron Lett.*, 2013, **54**, 594-599; J. Jia, K. Cao, P. Xue, Y. Zhang, H. Zhou and R. Lu, *Tetrahedron*, 2012, **68**, 3626-3632.

12 X. Cai, Y. Wu, L.Wang, N. Yan, J. Liu, X. Fang and Y. Fang, *Soft Matter*, 2013, **9**, 5807-5814; Y. Jiang, F. Zeng, R. Gong, Z. Guo, C. Chen and X. Wan, *Soft Matter*, 2013, **9**, 7538-7544; P. D. Wadhavane, M. A.Izquierdo, F. Galindo, M. I. Burguete and S. V. Luis, *Soft Matter*, 2012, **8**, 4373-4381.

13 Y. Xu, P. Xue, D. Xu, X. Zhang, X. Liu, H. Zhou, J. Jia, X. Yang, F. Wang and R. Lu, *Org. Biomol. Chem.*, 2010, **8**, 4289-4296.

14 M. Moniruzzaman and P. R. Sundararajan, *Langmuir*, 2005, **21**, 3802-3807.
15 X. Liu, X. Zhang, R. Lu, P. Xue, D. Xu and H. Zhou, *J. Mater. Chem.*, 2011, **21**, 8756-8765; X. Liu, Defang Xu, R. Lu, B. Li, C. Qian, P. Xue, X. Zhang and H. Zhou, *Chem. Eur. J.*, 2011, **17**, 1660-1669.
16 P. Xue, P. Chen, J. Jia, Q. Xu, J. Sun, B. Yao, Z. Zhang and R. Lu, *Chem. Commun.*, 2014, **50**, 2569-2571; W. Tian and J. Tian, *Dyes Pigments*, 2014, **105**, 66-74.
17 J. S. Yang, K. L. Liau, C. M. Wang, and C. Y. Hwang, *J. Am. Chem. Soc.*, 2004, 126, 12325.
18 J. R. Lakowicz, Principles of Fluorescence Spectroscopy, Springer, 2006.
19 H. Shi, L. Xu, Y. Cheng, J. He, J. Dai, L. Xing, B. Chen and L. Fang, *Spectrochimica Acta Part A*, 2011, **81**, 730-738.
20 B. Fugetsu, W. Han, N. Endo, Y. Kamiya and T. Okuhara, *Chem. Lett.*, 2005, **34**, 1218-1219; I. Hisaki, H. Shigemitsu, Y. Sakamoto, Y. Hasegawa, Y. Okajima, *Angew. Chem. Int. Ed.*, 2009, **48**, 5465-5469.
21 B. An, S. Kwon, S. Jung and S. Y. Park, *J. Am. Chem. Soc.*, 2002, **124**, 14410-14415; Y. Li, F. Li, H. Zhang, Z. Xie, W. Xie, H. Xu, B. Li, F. Shen, L. Ye, M. Hanif, D. Ma and Y. Ma, *Chem. Commun.*, 2007, 231-233.
22 C. Bao, R. Lu, M. Jin, P. Xue, C. Tan, T, Xu, G. Liu and Y. Zhao, *Chem Eur. J.*, 2006, **12**, 3287–3294.
23 P. Chen, R. Lu, P. Xue, T. Xu, G. Chen and Y. Zhao, *Langmuir*, 2009, **25**, 8395-8399; (b) X. Yang, Ran. Lu, H. Zhou, P. Xue, F. Wang, P. Chen and Y. Zhao, *J. Colloid Interface Sci.*, 2009, **339**, 527-532; K. Miyamoto, T. Sawada, H. Jintoku, M. Takashi, T. Sagawa and H. Ihara, *Tetrahedron Lett.*, 2010, **51**, 4666-4669; D. Xu, X. Liu, R. Lu, P. Xue, X. Zhang, H. Zhou and J. Jia, *Org. Biomol. Chem.*, 2011, **9**, 1523-1528; X. Li, X. Zhang, S. Ghosh and F. Wörthner, *Chem. Eur. J.*, 2008, **14**, 8074-8078; S. K. Samanta and S. Bhattacharya, *Chem. Eur. J.*, 2012, **18**, 15875–15885.
24 J. Clark, C. Silva, R. H. Friend and F. C. Spano, *Phys. Rev. Lett.*, 2007, **98**, 206406; C. E. Halkyard, M. E. Rampey, L. Kloppenburg, S. L. Studer-Martinez and U. H. F. Bunz, *Macromolecules*, 1998, **31**, 8655-8659.
25 J. Liu, J. Yan, X. Yuan, K. Liu, J. Peng and Y. Fang, *J. Colloid Interface Sci.*, 2008, **318**, 397-404; X. Yang, G. Zhang, D. Zhang and D. Zhu, *Langmuir*, 2010, **26**, 11720-11725.
26 B. An, D. Lee, J. Lee, Y. Park, H. Song, and S. Y. Park, *J. Am. Chem. Soc.*, 2004, **126**, 10232–10233; C. Bao, R. Lu, M. Jin, P. Xue, C. Tan, G. Liu and Y. Zhao, *Org. Biomol. Chem.*, 2005, **3**, 2508-2512; S. Y. Ryu, S. Kim, J. Seo, Y. Kim, O. Kwon, D. Jang and S. Y. Park, *Chem. Commun.*, 2004, 70-71; Y. Liu, J. W. Y. Lam, F. Mahtab, R. T. K. Kwok and B. Z. Tang, *Front. Chem. China*, 2010, **5**, 325-330; J. Seo, J. W. Chung, E.-H. Jo and S. Y. Park, *Chem. Commun.*, 2008, 2794-2796; Y. Qian, S. Li, Q. Wang, X. Sheng, S. Wu, S. Wang, J. Li and G. Yang, Soft Matter, 2012, **8**, 757-764; X. Wang, P. Duan and M. Liu, *Chem. –Asian J.*, 2014, **9**, 770–778;
27 Y. Hong, J. W. Y. Lam and B. Z. Tang, *Chem. Soc. Rev.*, 2011, **40**, 5361-5388.